FREEZING TIME PREDICTION FOR FILM PACKAGED FOOD

S.W. Chin and S.Y. Spotar*
Department of Process and Food Engineering, Faculty of Engineering, University Putra Malaysia, 43400 UPM Serdang, Selangor Darul Ehsan, Malaysia.
*Email: sergei@eng.upm.edu.my

ABSTRACT

A freezing process of the film packaged slab-shaped food was studied by modeling and experimentally. Food stuff temperature histories were determined by carrying out a freezing operation in an air-blast freezer. A freezing model was developed for an asymptotic case when film and food perform independently; thus, assuming the void between the food and the film are caused by appreciable food density change. Advanced model gives freezing time prediction that agrees reasonably well with the observed data.

***Keywords**: food freezing, packaging film, numerical simulation.*

INTRODUCTION

Freezing is a most common method for long-term preservation of foods and other biomaterials. The freezing time is needed in order to select and design a freezing process, and to establish refrigeration system capacity requirements. Freezing time of foods can be predicted approximately by either analytical methods or by numerical methods [1-6]. The accurate prediction of freezing time is complex because of the significant influence of the freezing process on thermophysical properties which is particularly manifested for foods with high moisture contents. Freezing process simulation to calculate process times can be a useful tool in designing or modifying existing equipments or product. However total freezing times only demonstrate part of the picture because the product quality not only depends on the freezing time but also depends on the freezing rate at various parts of the product and homogeneity of the freezing process. Hence for more advanced analysis of freezing processes it is useful to calculate complete temperature profiles at various locations in the food product.

In practice many products are being frozen as packaged products (sausages, chickens, meat mince etc.). For example, the preservation of chilled or frozen meat from possible contaminations is fulfilled by packaging on polystyrene trays and wrapping with plastic film [7]. When the food is packaged in boxes or the food material is tightly covered by a film of plastic the additional heat resistance affects the freezing process parameters. Therefore the main objective of this paper is to develop the model predicting freezing time for film packaged food with high moisture content.

Modelling and Simulation of a Freezing Process

Most typical applications can be covered by considering a slab, cylindrical and spherical geometries of food. It is assumed that the food freezing process is modeled by the solution of the following heat conduction equation:

$$\rho(T)\,c(T)\frac{\partial T(x,t)}{\partial t} = x^{-m}\frac{\partial}{\partial x}\left[x^{m}k(T)\frac{\partial T(T,x)}{\partial x}\right] + s(x,t,T) \tag{1}$$

where m = 0, 1, 2 for slab, cylindrical, spherical geometries of food consequently.

For a slab geometry the initial and boundary conditions are assumed as follows:

initial temperature of food at t = 0 is

$$T_0 = T(x,0); \quad 0 \le x \le L \tag{2}$$

boundary condition over the surface subjected to the convective heat transfer is

$$q = -k\left(\frac{\partial T}{\partial x}\right)_{x=L} = h(T_\infty - T); \quad x = L, \quad t > 0 \tag{3}$$

food bottom is considered thermo-insulated with

$$\frac{\partial T}{\partial x} = 0; \quad x = 0, \quad t > 0 \tag{4}$$

The water-ice transition substantially changes the thermophysical properties of food materials. The accuracy of freezing times prediction substantially depends upon the accuracy of the description of the thermophysical properties of the product, namely density, thermal conductivity and thermal capacity, specifically. There are different models predicting these food properties versus temperature and composition [8, 9]. Here we follow the typical approach developed for foods with high moisture content [8-10]. Solution of the equation (1) requires approximation of the thermal properties of the product with temperature change. For the case of a product covered by a film, the equation (1) has been numerically solved in the range [*L*, 0] film thickness included. Thermophysical properties of the entire slab are described by piecewise functions including the density, heat capacity, and thermal conductivity $\rho_{film}, c_{film}, k_{film}$ taken constant over the film interval $x_b < x < L$ and temperature dependent properties of food at the interval $0 < x \le x_b$.

Beef mince has been chosen as the typical food with high moisture content. Data on the lean beef compositions as well as the suitable composition based correlations were taken from literature [8-9, 11, 12]. Thermophysical properties of beef mince were described by the following relationships:

density
$$\rho(T) = \left[\frac{X_W(T)}{\rho_W} + \frac{X_I(T)}{\rho_I} + \frac{X_F}{\rho_F} + \frac{X_P}{\rho_P} + \frac{X_C}{\rho_C} + \frac{X_S}{\rho_S}\right]^{-1} \tag{5}$$

where ice fraction and water fraction are temperature dependent as

ice fraction:
$$X_I = 0 \text{ if } T \ge T_f$$
$$X_I(T) = (X_{TW} - X_B)\left[1 - \frac{T_f}{T}\right] \text{ if } T < T_f \tag{6}$$

liquid water fraction:
$$X_W(T) = X_{TW} - X_I(T) - X_B \tag{7}$$

where bound water is evaluated as
$$X_B = 0.01 X_S \tag{8}$$

Product freezing point T_f is calculated as:

$$T_f = \frac{1 - X_{TW}}{0.06908 - 0.439 \cdot X_{TW}} \tag{9}$$

where X_{TW} is product total (liquid water and ice) water content.

Beef mince heat conductivity is given by:

$$k(T) = \rho(T) \cdot \left[\frac{X_I(T)k_I}{\rho_I} + \frac{X_W(T)k_W}{\rho_W} + \frac{X_F k_F}{\rho_F} + \frac{X_P k_P}{\rho_P} \frac{X_C k_C}{\rho_C} + \frac{X_S k_S}{\rho_S}\right] \tag{10}$$

and product heat specific heat capacity is

$$c_{beef} = \frac{dH(T)}{dT} = X_{TW}c_W + X_F c_F + X_P c_P + X_S c_S + X_C c_C \qquad \text{if} \quad T \geq T_f \tag{11}$$

$$c_{beef} = X_F c_F + X_P c_P + X_C c_C + X_B c_W + c_W\left[X_W(T) + (T - T_f)\frac{dX_W(T)}{dT}\right] + c_I\left[X_I(I) + (T - T_f)\frac{dX_I(T)}{dT}\right] - \lambda\frac{dX_I(T)}{dT} \quad \text{if } T < T_f \tag{12}$$

Thus, for the entire slab thermophysical properties are piecewise with formal discontinuity at x_b separated food and film material.

Lean beef mince composition was taken as in Table 1.

Table 1: Beef mince composition [12]

Total Water content	Fat	Crude protein	Carbohydrate	Solids
71.7%	5.7%	21.6%	0%	1%

Thermophysical properties of the packaging film were taken as in Table 2:

Table 2: Thermophysical Properties of Selected Packaging Materials [13, 14]

Property	Packaging Material			
	Aluminium (Al)	Polyethylene (PE)	Polyester (PET)	Polypropylene (PP)
ρ, kg/m^3	2689	850	1400	913
c_p, J/kg·K	2700	1550	1172	1926
k, W/m·K	235	0.16	0.29	0.118

Matlab software package [15] including a *partial differential equations toolbox* has been utilized for temperature field numerical calculations. Specifically, *pdepe* solver was employed for numerical solution of the heat conduction equation. The solver gives solution of initial-value problems for systems of parabolic partial differential equations in one space variable *x* and time *t* of the form

$$c\left(x,t,u,\frac{\partial u}{\partial x}\right)\frac{\partial u}{\partial t} = x^{-m}\frac{\partial}{\partial x}\left(x^m f\left(x,t,u,\frac{\partial u}{\partial x}\right)\right) + s\left(x,t,u,\frac{\partial u}{\partial x}\right) \tag{13}$$

where m = 1, 2, 3 corresponds to slab, cylindrical, or spherical symmetries, respectively.

The problem specification, namely initial and boundary conditions and heat conduction equation component *c, f, s* in equation (13) were coded into appropriate Matlab functions. Original equation (1) is rewritten to satisfy the form (13). For convenience while employing the solver the *u* variable substitutes for temperature *T*, i.e. $u \equiv T$

Then the *c, f* and *s* terms in *pdepe* solver were identified as

$$\rho(T)c_{beef}(T) \equiv \rho(u)c_{beef}(u) \to c\,, \qquad k(T)\frac{\partial T}{\partial x} \equiv k(u)\frac{\partial u}{\partial x} \to f\,, \qquad s = 0 \tag{14}$$

and coded using (2) - (12) relationships.

EXPERIMENTAL PROCEDURE

Air blast freezing was carried out in an air-blast freezer (ARMFIELD FT36-C) at T_∞ = -35°C with airflow parallel to the slab-shaped product surface at a velocity of about 10m/s. The schematic diagram of food freezing experiments is shown in Fig.1. Beef mince was congregated into slab-shaped samples of 6, 13, and 26 mm thicknesses. A K-type thermocouple (TP-K01 Wire Probe) was located at the food sample bottom as depicted in Fig.1. Thermocouple wire was assembled along the base line to prevent inaccuracy due to heat flux. The temperature changes with time were measured by the thermocouple and the data were collected by a digital data logger (Monarch 309) with a reading accuracy of ± 0.2°C. During the experiments, temperature changes were recorded in every 60 seconds intervals.

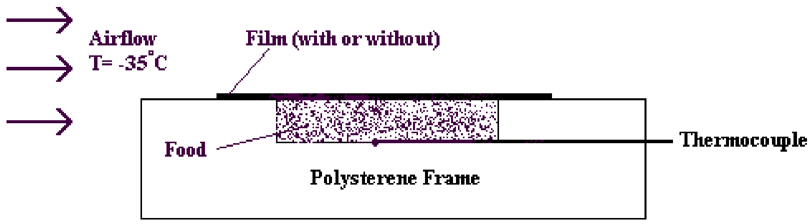

Figure 1: Schematic diagram for an air-blast freezing.

The convective heat transfer coefficient h was determined from the temperature history of the aluminium block subjected to the same conditions as the treated minced beef (standard lump capacity method). The value of $h \cong$ 90 W/m^2·K was obtained from the slope of a plot of the following equation

$$\ln T^* = \ln \frac{T - T_\infty}{T_0 - T_\infty} = -\frac{hA}{M_{Al}\, c_{Al}} t \tag{15}$$

The freezing time is the time required to reduce the initial product temperature to some established final temperature at the slowest cooling location [8]. In this study, the final established temperature was set as -35°C, while the slowest cooling location was at the bottom surface of the beef mince slab. Beef mince water content was determined by drying the sample at 105°C. It was found that ≈ 72 % that is in agreement with the data in Table 1.

The effect of freezing time delay for packaged slab-shaped products were studied in the series of experiments with the top surface of the beef mince was covered by different packaging films.

RESULTS AND DISCUSSION

Figure 2, a simulated temperature curves for unpackaged food (sample top surface is opened to cooling air) are in good agreement with the experimental data obtained for the slabs of different thicknesses.

The delay of the freezing time caused by imposed packing film additional thermal resistance is shown in Figure 3. The temperature histories for the food sample of the same thickness (13 mm) become differentiated depending on the packing films thermal conductivity and thickness. Thus, as expected for the thin aluminium (k = 235 W/m·K) foil, there is no appreciable difference in the product freezing history comparing with unpackaged food sample, on the other hand, 0.43 mm polypropylene film increases the product freezing time twice.

To quantitatively predict the presented freezing time delay, the effect of the film covered the product surface was considered. An overall heat transfer coefficient concept, i.e. the convective heat transfer coefficient h was substituted by an appropriate overall heat transfer coefficient U determined as

$$U = \frac{1}{\dfrac{1}{h} + \dfrac{\delta_{film}}{k_{film}}} \tag{16}$$

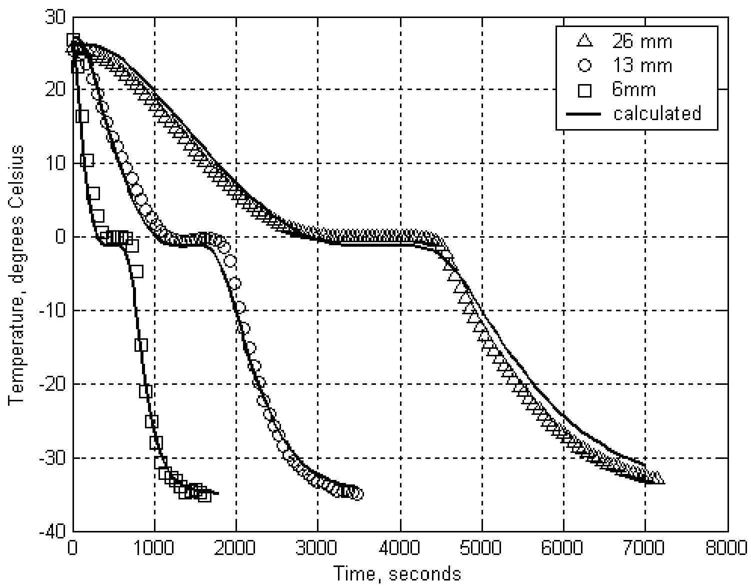

Figure 2: Effect of the sample thickness (L = 6mm, 13 mm, 26 mm) on temperature histories of the beef mince slabs frozen in an air blast freezer.

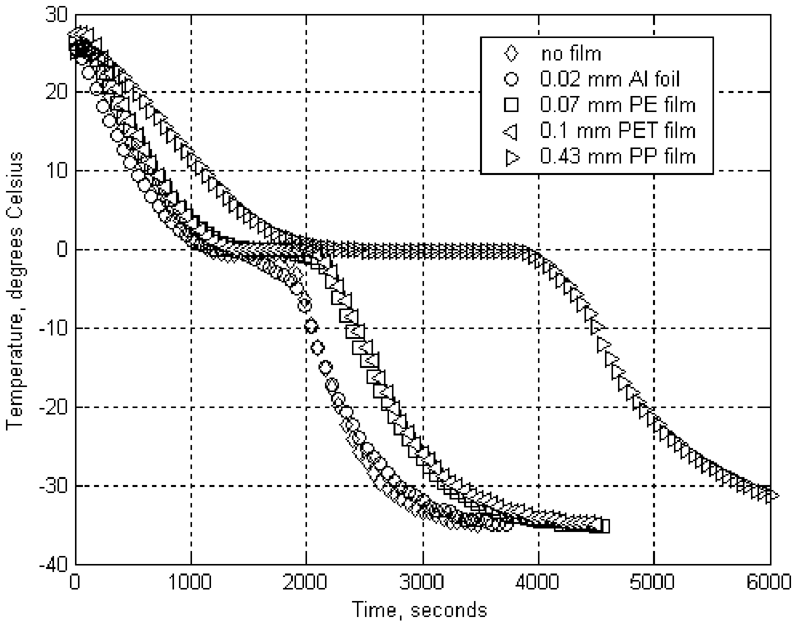

Figure 3: Experimental temperature histories of the beef mince slab (δ_b = 13mm) covered with different types of packaging films.

In the second approach the slab was assumed as a composite consisting of the food and film layers, and piecewise functions were applied to describe the combined thermal properties of the slab. Both methods brought very close temperature history curves that rather indicate freezing time delay tendency but do not satisfy the experimental data. The process modeling results are given in Figure 3.

It is worth to point out that, the perfect mechanical and thermal contact between food sample and film were assumed. Non-perfect contact between food and film normally increases thermal resistance due to cavities, roughness, surface irregularities etc. The fitting experimental data curve 4 was simulated when actual film thermal conductivity was replaced by an apparent empirical thermal conductivity value reflecting non-ideal contact between food and film. For this reason, the matching curve 4 does not manifest a model prediction capacity of the effect but rather consolidates the effect connection with non-perfect contact.

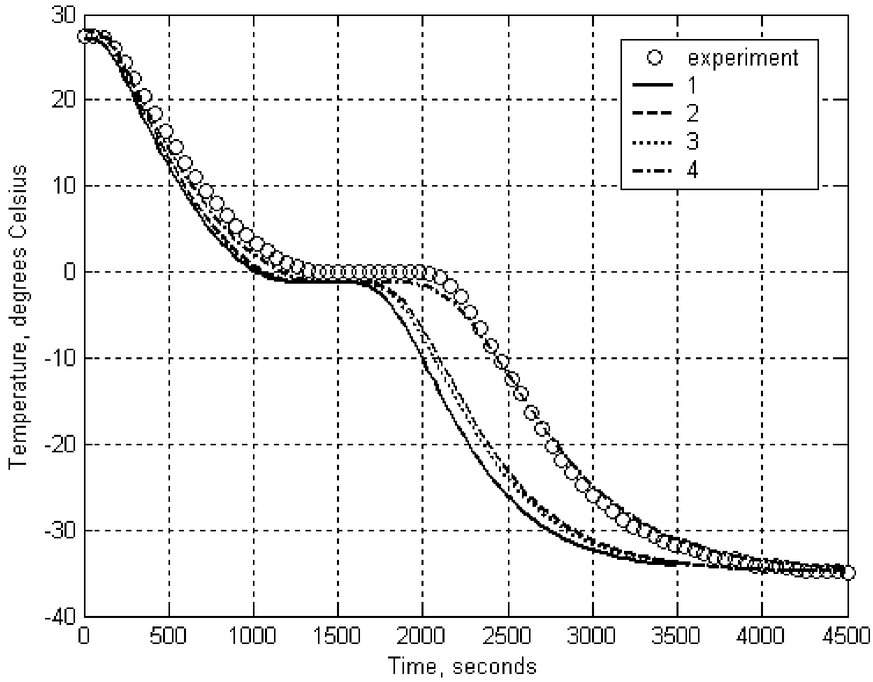

Figure 4: Simulated and experimental temperature histories of 13 mm beef mince slab packaged with 0.1 mm PET film. Curves: 1 – no film; 2 – using overall heat transfer coefficient; 3 – using piecewise conductivity, perfect thermal contact; 4 – using apparent film thermal conductivity k = 0.04 W/m·K (non-perfect thermal contact).

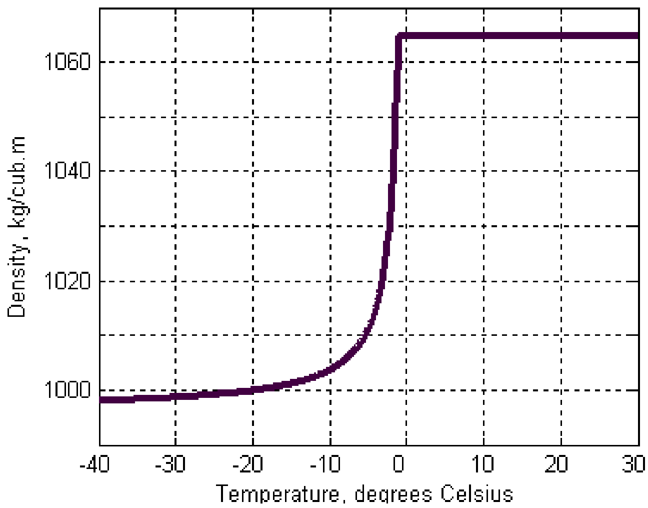

Figure 5: Beef mince density calculated from equation (5).

There are many factors associated with possible thin film and food such as film elasticity, food surface profile etc., that determine of the actual thermal resistance Rapid thermal expansion of the food with high moisture content near freezing point (Figure 5) could be the main reason for non-perfect contact however this mechanism is not sole in practice.. Generally it is problematic to model the mechanism of the non-perfect thermal contact and to predict the appropriate thermo-physical properties of the media due to many uncertainties such as the ability of the thin film to follow the food stuff etc. We assume, however that, utilizing comparatively thick rigid film, the asymptotic case takes place when the food stuff and the film can be considered behaving independently. In this study specifically 0.43 mm PP film was assumed quite rigid to be deformed by the extended food. In the asymptotic case we presume that the gap between food and film can be evaluated as the result of beef mince expansion due to its density change with temperature while the density of the plastic material is nearly constant. A linear expansion coefficient of the beef mince can be assumed as $\left(\frac{\rho(T_0)}{\rho(T_\infty)}\right)^{\frac{1}{3}}$, then the gap due to the thermal expansion is estimated as

$$\delta_{air} \approx \left(\frac{\rho(T_0)}{\rho(T_\infty)}\right)^{\frac{1}{3}} \delta_b \tag{17}$$

In the case considered relationship (17) results in 0.29 mm gap space between 13 mm beef sample and film. Further we assigned the air physical properties to this gap and proceeded with calculations of temperature fields, by modifying the model introducing new piecewise functions for density, thermal capacity and thermal conductivity. Thus for an asymptotic non-perfect thermal contact, the same equation (1) has been numerically solved in the range [*L*,0] film and gap thicknesses included. Thermophysical properties of the entire slab are described by piecewise functions consisting of the density, heat capacity, and thermal conductivity $\rho_{film}, c_{film}, k_{film}$ and $\rho_{air}, c_{air}, k_{air}$ taken constant at the film $x_{film} < x < L$ and air gap $x_b < x < x_{film}$ intervals consequently and temperature dependent properties of food at the interval $0 < x \le x_b$. Alternatively, the overall heat transfer coefficient concept was applied to investigate the effect of asymptotic non-perfect contact as follows:

$$U = \frac{1}{\frac{1}{h} + \frac{\delta_{film}}{k_{film}} + \frac{\delta_{air}}{k_{air}}} \tag{18}$$

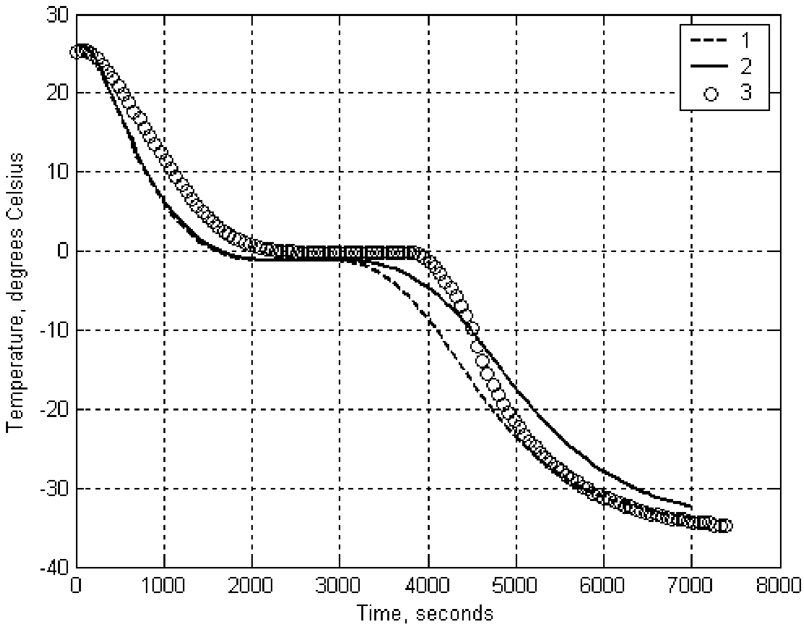

Figure 6: Calculated and experimental temperature histories of beef mince packaged with 0.43 mm PP film. Curves: 1 – using overall heat transfer coefficient; 2 – using piecewise conductivity, perfect thermal contact; 3 – experimental data.

Results of the food bottom temperature simulation for the asymptotic case were compared with the experimental curve as given in Figure 6. Simulated curves slightly deviate from experimental data but are positioned quite closely to the observation for the practical-need accuracy. Curves 1 and 2 both give close prediction for the food bottom temperature development; however the temperature profiles development across the slab should be analyzed using a piecewise slab presentation approach. Such data in Figure 7 and 8 give the integral picture of the freezing process and reflect explicitly the boundary effects caused by the film.

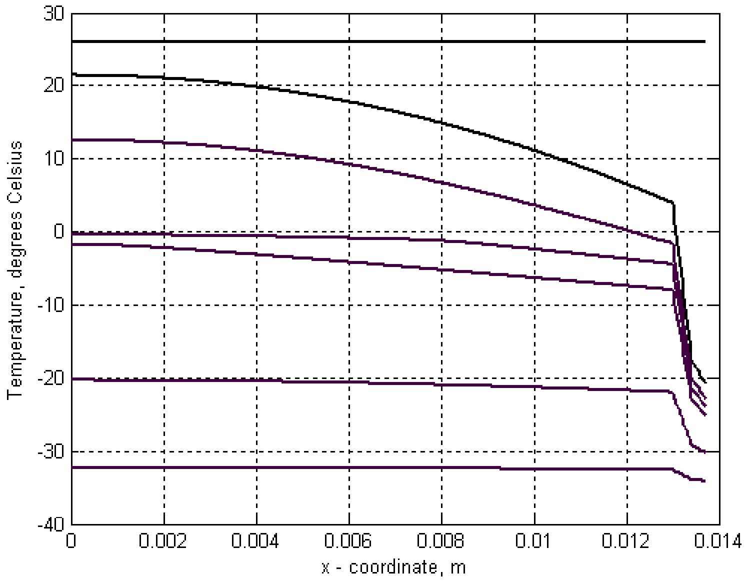

Figure 7: Simulated temperature profiles at t = 0, 350, 700, 1750, 3500, 5250, 7000 s for freezing of beef mince covered with 0.43 mm PP film.

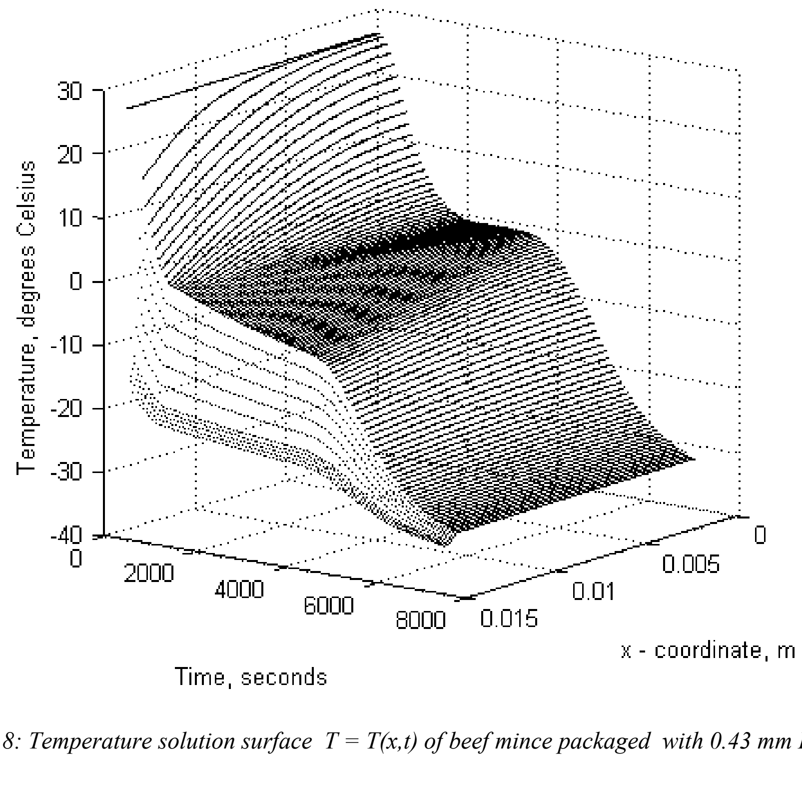

Figure 8: Temperature solution surface T = T(x,t) of beef mince packaged with 0.43 mm PP film.

CONCLUSIONS

It was found that the observed freezing time was appreciably greater for film covered product than expected, if the perfect thermal contact between film and food occurred. A freezing model was developed for an asymptotic case when film and food perform independently by assuming that the air gap between food and film are caused by temperature expansion. Modification gives freezing time prediction that agrees reasonably well with the observed data.

NOMENCLATURE

A surface area [m^2]
c heat capacity [J / kg K]
h heat transfer coefficient [W / m^2 K]
U overall heat transfer coefficient [W / m^2 K]
H enthalpy [J / kg]
k thermal conductivity [W / m K]
λ latent heat of fusion [J / kg]
ρ density [kg / m^3]
t time [s]
T temperature [°C]
T_f food freezing temperature [°C]
T_0 initial food temperature [°C]
T_∞ bulk temperature of the air stream [°C]
δ thickness [m]
L entire slab thickness [m]
X component mass fraction
M mass [kg]
m space index
b, W, I, F, P, C, S beef, water, ice, fat, protein, carbohydrates, solids indexes

REFERENCES

[1] Cleland, A.C. (1990) Food refrigeration processes: analysis, design and simulation: 284, Elsevier Applied Science, London.

[2] Delgado, A.E., Sun, D.W. (2001) Heat and mass transfer models for predicting freezing processes – a review. Journal of Food Engineering **47**: 157 – 174.

[3] Cleland, D.J., Cleland, A.C., Earle, R.L. and Byrne, S.J., (1987) Prediction of freezing and thawing times for multi-dimensional shapes by numerical methods. International Journal of Refrigeration **10**: 32–39.

[4] Ilicali, C., Cetin, M. and Cetin, S., (1996) Methods for the freezing time of ellipses. Journal of Food Engineering **28**: pp. 361–372.

[5] Pham, Q.T., (1986) Simplified equation for predicting the freezing time of foodstuffs. Journal of Food Technology **21**: 209–219.

[6] Ansari F.A., Charan V., Varma H.K. (1985) Measurement of thermophysical properties and analysis of heat transfer during freezing of slab-shaped food commodities. International Journal of Refrigeration **8** (2): 85-90.

[7] Cannarsi, M., Baiano A., Marino R., Sinigaglia M., Del Nobile M.A.(2005). Use of biogradable films for fresh cut beef steaks packaging. Meat Science **70**(2): 259 – 265.

[8] Heldman, D.R. (1992) Food freezing. In D.R. Heldman & D.B. Lund (Eds.) Handbook of food engineering: 756, Marcel Dekker, New York .

[9] Kenneth, J.V., Enrique R., Singh H.P. (1997) Handbook of food engineering practice: 718, CRC Press, Boca Raton, Florida.

[10] Spotar S.Y., Ibrahim M.N., Nor Amaiza N.A.M. (2002) Modelling and experimental study of keropok lekor freezing process. Proceeding of 2nd World Engineering Congress: 173-177, University Putra Malaysia Press, Serdang.

[11] Mohsenin N.N. (1979). Thermal properties of foods and agriculture materials: 407, Gordon and Breach Science Publishers, New York.

[12] Wahrmund-Wyle J.L., Harris K.B., Sawell W. (2000). Beef retail cut composition: 2. Proximate Analysis. Journal of food composition and analysis **13**(3): 243 – 251.

[13] Van Krevelen, D.W. (1990). Properties of polymers: their correlation with chemical structure; their numerical estimation and prediction from additive group contributions: 430, Elsevier Scientific Publishing, Amsterdam.

[14] Specifications on Questar™ polyester film. (2006). http://www.petfilm.com/specifications.html#1

[15] MATLAB Users Guide (2005) The MathWorks Inc., Natick, MA.